



## Molecular Gas Sensing Below Parts Per Trillion: Radiocarbon-Dioxide Optical Detection

I. Galli, S. Bartalini, S. Borri, P. Cancio,\* D. Mazzotti, P. De Natale, and G. Giusfredi

*Istituto Nazionale di Ottica-CNR (INO-CNR)<sup>†</sup> and European Laboratory for Non-Linear Spectroscopy (LENS)<sup>‡</sup> Via N. Carrara 1, I-50019 Sesto Fiorentino, Italy*

(Received 17 May 2011; published 30 December 2011)

Radiocarbon ( $^{14}\text{C}$ ) concentrations at a 43 parts-per-quadrillion level are measured by using saturated-absorption cavity ringdown spectroscopy by exciting radiocarbon-dioxide ( $^{14}\text{C}^{16}\text{O}_2$ ) molecules at the  $4.5\ \mu\text{m}$  wavelength. The ultimate sensitivity limits of molecular trace gas sensing are pushed down to attobar pressures using a comb-assisted absorption spectroscopy setup. Such a result represents the lowest pressure ever detected for a gas of simple molecules. The unique sensitivity, the wide dynamic range, the compactness, and the relatively low cost of this table-top setup open new perspectives for  $^{14}\text{C}$ -tracing applications, such as radiocarbon dating, biomedicine, or environmental and earth sciences. The detection of other very rare molecules can be pursued as well thanks to the wide and continuous mid-IR spectral coverage of the described setup.

DOI: [10.1103/PhysRevLett.107.270802](https://doi.org/10.1103/PhysRevLett.107.270802)

PACS numbers: 07.07.Df, 33.20.Ea, 42.62.Eh, 87.64.km

Tackling critical challenges like global climate changes, energy plant monitoring, or detection of hazardous substances for homeland security sometimes requires quantitative measurements of extremely small amounts of molecular gases. Trace gas detection by optical spectroscopy plays a key role in such measurements and, more generally, allows us to gain knowledge about physical, chemical, and biological processes. A privileged window for ultrasensitive molecular spectroscopy is the so-called fingerprint region ( $2.5$  to  $10\ \mu\text{m}$ ) of the infrared (IR) spectrum, where the strongest absorption lines can be excited [1]. Well-assessed trace gas sensing techniques for the visible and near-IR are now being extended to the mid-IR, thanks to the growing number of powerful, stable, and tunable coherent sources [2–4]. In particular, their combination with optical frequency comb synthesizers (OFCSs) [5–7] has improved frequency stability [8] and detection sensitivity [9]. Presently, molecular concentration measurements are limited to the parts-per-trillion (ppt) range, even when the strongest rovibrational molecular absorptions in the fingerprint region are targeted [10–12]. Such a limitation has prevented optical detection of rare-isotope-containing molecules, due to the very low abundance of such species. Among them, concentration measurements down to parts per billion of ubiquitous long-lived radioisotopes are relevant in a broad range of scientific and technological fields [13,14]. In particular, nature marks every living being with a specific isotope,  $^{14}\text{C}$ , which has acquired great importance after the discovery of the radiocarbon dating method [15] in the early 1950s. Radiocarbon, produced in the upper atmosphere by secondary cosmic rays, has a natural abundance  $^{14}\text{C}/\text{C} \approx 1.2 \times 10^{-12}$ . Because of its historical-scale radioactive half-life (about 5730 years), it is an ideal marker for age assessment of samples of biological origin [16]. At present, high energy accelerator mass spectrometry (AMS), with

$^{14}\text{C}/^{12}\text{C}$  sensitivity hitting  $10^{-15}$ , represents the only method capable of dating very old samples (about 50 000 years), at the price of big size, cost, and complexity of the instrumentation [17]. Apart from dating, radiocarbon detection has become an essential tool in modern science, such as biomedicine [16] or environmental and earth sciences [18]. AMS technology is also used for these applications but with more relaxed sensitivity requirements. Laser spectroscopy detection of such an isotope targets simple  $^{14}\text{C}$ -containing molecules, in particular,  $^{14}\text{C}^{16}\text{O}_2$ . Recently, measurement of the  $^{14}\text{C}/^{12}\text{C}$  ratio at the natural abundance level was reported by using intracavity optogalvanic spectroscopy [19]. The narrow dynamic range ( $^{14}\text{C}/^{12}\text{C} \approx 2 \times 10^{-12}$  to  $10^{-15}$ ) and calibration problems of such a method limit its practical deployment in radiocarbon-based applications, including dating. Attempts to use absorption laser spectroscopy [20,21] targeted fundamental rovibrational transitions of the  $^{14}\text{C}^{16}\text{O}_2$  molecule around the  $4.5\ \mu\text{m}$  wavelength, but detection sensitivity was insufficient, mostly due to the lack of suitable tunable lasers and techniques. Here, we report on radiocarbon optical detection well below natural abundance ( $^{14}\text{C}/\text{C} = 4.3 \times 10^{-14}$ ), in  $\text{CO}_2$ , by exploiting saturated-absorption cavity ringdown (SCAR) spectroscopy [9] at the  $4.5\ \mu\text{m}$  wavelength, in combination with our recently developed OFCS-referenced high-power mid-IR coherent source [3]. Following the first demonstration of the SCAR technique [9], in the present Letter, we push on full exploitation of its ultimate sensitivity by detecting the elusive  $^{14}\text{C}^{16}\text{O}_2$  molecule at concentrations down to 43 parts per quadrillion (ppq). This result opens new scenarios for dating and other radiocarbon-based applications with a compact and relatively low-cost setup. In addition, the wide and continuous mid-IR spectral coverage of the proposed apparatus provides very broad applicability for molecular trace gas detection.

In our experiment, the  $(00^01 - 00^00)$   $P(20)$  rovibrational transition of  $^{14}\text{C}^{16}\text{O}_2$  around  $4.5 \mu\text{m}$  was targeted for SCAR spectroscopy. The apparatus, schematically shown in Fig. 1, is simple, as in cavity ringdown spectroscopy.  $\text{CO}_2$  gas inside a high-finesse Fabry-Perot cavity (FPC) absorbs resonant IR radiation, delivered by a difference-frequency-generation (DFG) process inside a Ti:Sapphire laser cavity [3]. When the cavity is filled up to a threshold level, the IR light is quickly switched off-resonance and photons leaking out of the cavity are detected. Saturated absorption for intracavity light intensities much larger than the saturation intensity of the targeted molecular transition allows us to decouple the linear gas absorption rate,  $\gamma_g$ , from other cavity losses,  $\gamma_c$ , and to independently measure them for each SCAR event, as described in [9]. At the  $\text{CO}_2$  pressures of the present measurements, saturation of the  $^{14}\text{C}^{16}\text{O}_2$   $P(20)$  transition is dominated by homogeneous collisional broadening and velocity-changing collisions, and therefore with an absorption coefficient approximated by

$$\alpha(t; \Delta\nu) = \frac{\alpha_0 g(\Delta\nu)}{1 + \frac{I(t)}{I_s} g(\Delta\nu)}, \quad (1)$$

where  $\alpha_0$  is the nonsaturated absorption at resonance,  $g(\Delta\nu)$  is a Voigt function normalized to 1 on the peak,  $\Delta\nu$  is the detuning from resonance, and  $I(t)$  and  $I_s$  are the laser intensity and the saturation intensity, respectively. Thus, the integration of Eq. (1) on the intracavity Gaussian laser beam profile gives the differential power decay for each detuning

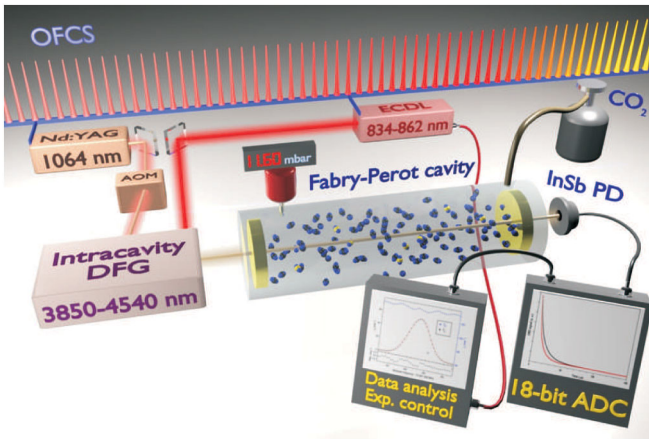


FIG. 1 (color). Schematics of the experimental setup. The IR radiation, tunable between 3850 and 4540 nm, is delivered by a DFG process inside a Ti:Sapphire laser cavity. The Ti:Sapphire laser, optically injected by an external-cavity diode laser (ECDL), and a Nd:YAG laser are mixed in a nonlinear crystal. Both lasers, and hence the IR radiation, are frequency-locked to the OFCS. After switching off-resonance the IR radiation by an acousto-optic modulator (AOM), the light transmitted by a Fabry-Perot cavity is detected by an InSb photodiode (PD). The signal is acquired by an analog-to-digital converter (ADC).

$$\frac{dG}{dt} = -\gamma_c G - \gamma_g \ln(1 + G), \quad (2)$$

where  $G$  is the saturation function

$$G(t; \Delta\nu) = P(t) \frac{g(\Delta\nu)}{P_s} = P(t) U_s(\Delta\nu), \quad P_s = \frac{\pi w^2}{2} I_s, \quad (3)$$

$P(t)$  is the intracavity power,  $\gamma_g = c\alpha_0 g(\Delta\nu)$ , and  $w$  is the beam waist. Hence, we measured  $\gamma_g$  at each IR laser frequency by fitting each SCAR-decay curve, taking into account Eq. (2), numerically integrated according to the procedure described in [9]. OFCS-DFG phase lock [8] provides absolute and reproducible synthesis of the generated IR frequency. As a consequence, precise IR frequency scans with a Cs frequency standard traceability can be performed. An average of several consecutive and identical scans (each one with an up and down frequency change) was used to increase the signal-to-noise ( $S/N$ ) ratio of the recorded spectrum.

We show in Fig. 2 a spectrum of the  $^{14}\text{C}^{16}\text{O}_2$   $P(20)$  transition (black trace) recorded at the present natural abundance (named “2010” in this Letter). In this figure, two more spectra are shown, corresponding to a  $^{14}\text{C}$ -enriched sample (green trace) and a  $^{14}\text{C}$ -depleted sample (blue trace).  $^{14}\text{C}$ -enriched spectra were used to accurately measure the center frequency of the  $P(20)$  transition, as well as the most favorable thermodynamic conditions of the gas sample for  $^{14}\text{C}$  detection in subnatural abundance. From such an analysis, we chose dry-ice temperature (195 K) and a pressure of 11.60(2) mbar as a trade off to

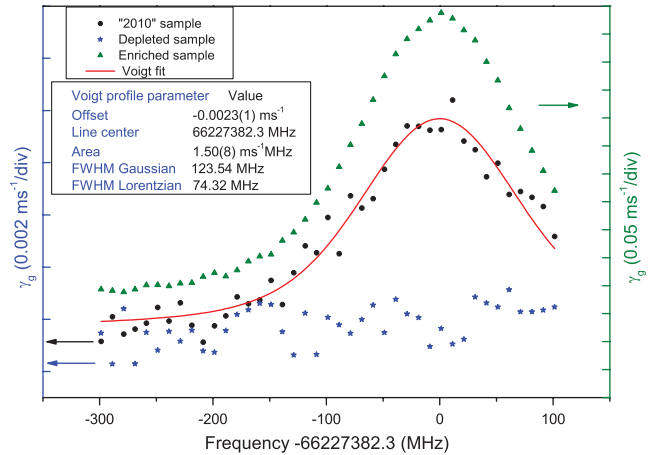


FIG. 2 (color). SCAR radiocarbon-dioxide ( $^{14}\text{C}^{16}\text{O}_2$ ) spectra of the  $(00^01 - 00^00)$   $P(20)$  rovibrational transition around  $4.5 \mu\text{m}$  for three different samples. Green trace:  $^{14}\text{C}$ -enriched (about 58 times)  $\text{CO}_2$  (one scan, right vertical scale). Black trace: 2010  $\text{CO}_2$ , and blue trace:  $^{14}\text{C}$ -depleted  $\text{CO}_2$  (thirty-two scans, left vertical scale in both cases). Red line: Voigt fit of the 2010 spectrum with area and offset as free parameters, while keeping the line center and linewidths (full width at half maximum, FWHM) fixed to the values obtained for the  $^{14}\text{C}$ -enriched spectrum. The gas temperature and pressure were 195 K and 11.60(2) mbar, respectively.

achieve both a strong absorption signal and an initial saturation level  $G_0 = P(0)U_S$  of about 30. At the same time, interferences from other  $\text{CO}_2$  lines were minimized [20]. The 400-MHz redshifted scan width was chosen in order to get the highest  $S/N$  ratio in the shortest acquisition time. The well-defined wing and signal points provide, after data fitting, an unambiguous line profile determination and hence an accurate estimation of the area under the line shape.

The black trace in Fig. 2 represents the first all-optical detection of a radiocarbon-marked molecule in natural abundance. It belongs to the 2010  $\text{CO}_2$  sample, produced from recent biological material [22], and a spectral signal above the noise level is clearly recorded. Instead, a signal indistinguishable from the noise level was detected for a highly  $^{14}\text{C}$ -depleted  $\text{CO}_2$  sample, as shown in the blue trace. More quantitatively, the fit of the 2010  $\text{CO}_2$  spectrum to the expected Voigt profile yields an area of  $1.50(8) \text{ ms}^{-1} \text{ MHz}$ . Assuming for the  $P(20)$  the calculated line strength,  $S = 3.10(15) \times 10^{-18} \text{ cm}$  [23], we measure a  $^{14}\text{C}^{16}\text{O}_2$  natural abundance concentration of 1.24(10) ppt, in agreement with the present natural abundance of 1.235(14) ppt [24].

By mixing the 2010  $\text{CO}_2$  gas sample with the  $^{14}\text{C}$ -depleted one, we estimated the ultimate detection sensitivity of our setup, as shown in Fig. 3. The agreement between the fitted line and the experimental data within 1 standard deviation demonstrates the truly linear response of the SCAR method, throughout the ancient to 2010  $\text{CO}_2$  concentration range. We estimate the actual minimum detectable concentration of  $^{14}\text{C}^{16}\text{O}_2$  by calculating the uncertainty of the linear fit at the present natural abundance (100% of 2010  $\text{CO}_2$ ), which is 43 ppq. The resulting molecular density is  $1.9 \times 10^4 \text{ cm}^{-3}$ , which corresponds to a minimum detectable pressure of  $5 \times 10^{-16} \text{ bar}$ . Therefore, we measure  $^{14}\text{C}/^{12}\text{C}$  ratios in the present natural abundance samples with an accuracy of 3.5% in 1 h of averaging, which is about 1 order of magnitude worse than the best AMS isotopic ratio uncertainty with the same acquisition time. Such a result demonstrates the applicability of our radiocarbon detection method to fields like biomedicine [16], where a  $^{14}\text{C}$  detection accuracy of about 5% is required. Moreover, biomedical applications also demand a wider dynamic measurement range ( $^{14}\text{C}/^{12}\text{C} \approx 10^{-9}$  to  $10^{-12}$ ), which is fulfilled by the present SCAR setup, since gas concentrations with  $\gamma_g$  as high as  $\gamma_c$  can be measured. Furthermore, since the  $^{14}\text{C}^{16}\text{O}_2$  molecules are not destroyed during interaction with light, the SCAR samples could be remeasured by other methods, such as AMS, for cross calibration or comparison purposes [25].

In the inset of Fig. 3, the equivalent ages corresponding to the mixing ratios are reported. Possible systematic errors affecting the measured  $^{14}\text{C}^{16}\text{O}_2$  concentration have not yet been fully investigated. Although we are confident that they are negligible at the current sensitivity level, they prevent us from estimating a true age. Since the present

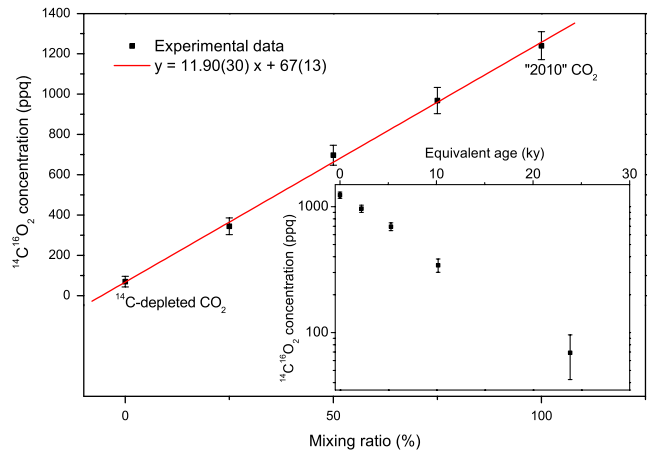


FIG. 3 (color online). Radiocarbon-dioxide detection linearity and sensitivity. Linear behavior of the measured  $^{14}\text{C}^{16}\text{O}_2$  concentration vs its trace content in  $\text{CO}_2$  gas samples ranging from ancient to 2010. All data are the results of a 32-scan average, acquired in 1 h. The samples were obtained by a controlled mixing of the 2010  $\text{CO}_2$  gas with the  $^{14}\text{C}$ -depleted one, while keeping the total pressure constant at 11.60(2) mbar. In the inset graph, such measurements are plotted in terms of equivalent age of the  $\text{CO}_2$  gas, by considering 0 years the present age and an infinite age for a  $\text{CO}_2$  sample without  $^{14}\text{C}^{16}\text{O}_2$ .

limiting noise source due to spurious nonlinearities in the SCAR signals is “white,” further averaging improves the  $S/N$  ratio, thus providing access to older dates. We are working to minimize the dead time between SCAR events, so as to improve sensitivity without increasing acquisition time. Increasing the FPC finesse with higher-reflectivity mirrors would improve sensitivity as well. Another parameter to be improved for future dating applications is the minimum measurable radiocarbon content. For the present measurements, the total C mass in the sample gas was about 68 mg. A reduction of the C content of the samples down to the level of AMS graphite tablets ( $\approx 3 \text{ mg}$ ) can be achieved by reducing the size of the vacuum chamber enclosing the FPC.

The sensitivity of a trace gas detection method can be expressed in terms of the minimum detectable pressure of a given molecular species (in units of  $\text{mbar}/\text{Hz}^{1/2}$ ). This definition allows us to compare and rank different methods, based on different spectroscopic techniques, spectral ranges, sources, and detectors. Figure 4 shows a collection of the best ever published sensitivities, labeled by molecular species, wavelength, and technique [10–12,26–31]. From such a comparison,  $\text{CO}_2$  detection with the SCAR technique results to be the most sensitive, with detected molecular gas pressures, in a 1-Hz bandwidth, of a few tens of femtobar. The sensitivities of the closest determinations are about 3 times worse.

In conclusion, optical detection of radiocarbon-containing  $\text{CO}_2$ , well below its subnatural abundance, has been demonstrated by using SCAR spectroscopy. Moreover, unlike AMS and intracavity optogalvanic spec-



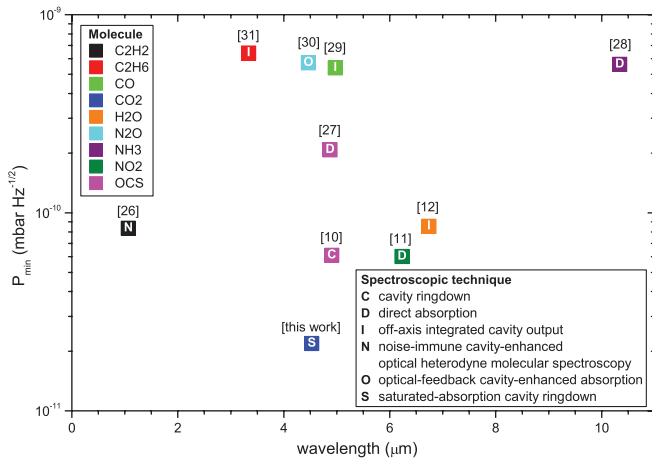


FIG. 4 (color). Molecular trace gas sensitivity ranking graph with the best sensitivities achieved by using the molecular absorption spectroscopy in the IR spectral range. The minimum detectable pressures (up to  $10^{-9}$  mbar Hz $^{-1/2}$ ) are related to 9 different molecular species (color) and 6 different laser absorption techniques (letter). For all these data, the noise-equivalent absorbance for the strongest transition of the detected molecule at the given wavelength was calculated. References are given in brackets.

troscopy methods, in which only a  $^{14}\text{C}$  abundance relative to  $^{12}\text{C}$  ( $^{14}\text{C}/^{12}\text{C}$  ratio) can be measured, absolute concentrations are retrieved with the SCAR-based technique, with a superior dynamic range and without any sample degradation. The present table-top setup represents a valid analysis method of  $^{14}\text{C}$ -marked samples, alternative to those presently used in such applications as biomedicine, and represents a major step towards an optical radiocarbon detection method for dating. Finally, the minimum detectable pressure of a few hundred attobars measured for  $\text{CO}_2$  sets a new benchmark for trace gas detection, and the wide tunability of the reported setup allows us to extend similar sensitivity levels to a large number of molecules.

We thank V. Perevalov, V.E. Zuev Institute of Atmospheric Optics–Russian Academy of Science, for calculating molecular data and M. Fedi, University of Firenze and INFN, for discussions about AMS dating. We gratefully acknowledge Michele Giusfredi for his support in the 2010  $\text{CO}_2$  gas preparation. This work was partially supported by Ente Cassa di Risparmio di Firenze and by Regione Toscana through the project CTOTUS, in the framework of POR-CReO 2007-2013.

\*pablo.canciopastor@ino.it

†http://www.ino.it

‡http://www.lens.unifi.it

- [1] L. S. Rothman *et al.*, *J. Quant. Spectrosc. Radiat. Transfer* **110**, 533 (2009).  
 [2] J. Faist *et al.*, *Science* **264**, 553 (1994).  
 [3] I. Galli *et al.*, *Opt. Lett.* **35**, 3616 (2010).

- [4] E. Andrieux *et al.*, *Opt. Lett.* **36**, 1212 (2011).  
 [5] T. Udem, J. Reichert, R. Holzwarth, and T. W. Hänsch, *Phys. Rev. Lett.* **82**, 3568 (1999).  
 [6] S. A. Diddams *et al.*, *Phys. Rev. Lett.* **84**, 5102 (2000).  
 [7] P. Maddaloni, P. Cancio, and P. De Natale, *Meas. Sci. Technol.* **20**, 052001 (2009).  
 [8] I. Galli *et al.*, *Opt. Express* **17**, 9582 (2009).  
 [9] G. Giusfredi *et al.*, *Phys. Rev. Lett.* **104**, 110801 (2010).  
 [10] D. Halmer, G. von Basum, P. Hering, and M. Mürtz, *Opt. Lett.* **30**, 2314 (2005).  
 [11] B. H. Lee *et al.*, *Appl. Phys. B* **102**, 417 (2011).  
 [12] E. J. Moyer *et al.*, *Appl. Phys. B* **92**, 467 (2008).  
 [13] Z.-T. Lu and K. D. A. Wendt, *Rev. Sci. Instrum.* **74**, 1169 (2003).  
 [14] W. Jiang *et al.*, *Phys. Rev. Lett.* **106**, 103001 (2011).  
 [15] J. R. Arnold and W. F. Libby, *Science* **113**, 111 (1951).  
 [16] H.-A. Synal and L. Wacker, *Nucl. Instrum. Methods Phys. Res., Sect. B* **268**, 701 (2010).  
 [17] Our setup has an overall cost of 300 k Euro and a  $\sim 2$  m $^2$  footprint about 1 and 2 orders of magnitude, respectively, less than the best AMS facilities.  
 [18] I. Levin *et al.*, *Tellus, Ser. B, Chem. Phys. Meteorol.* **62**, 26 (2010).  
 [19] D. Murnick, O. Dogru, and E. Ilkmen, *Nucl. Instrum. Methods Phys. Res., Sect. B* **268**, 708 (2010).  
 [20] D. Labrie and J. Reid, *Appl. Phys. A* **24**, 381 (1981).  
 [21] R. L. Sams and J. R. DeVoe, *J. Mol. Spectrosc.* **128**, 296 (1988).  
 [22] The 2010  $\text{CO}_2$  sample was obtained by  $\text{CO}_2$  gas distillation as a product of brown cane sugar fermentation. The cane sugar produced in a region of the Earth far from anthropic pollution (the Paraguayan Manduvira cultivation) is distributed by the World Fair Trade Organization.  
 [23] V. Perevalov (private communication).  
 [24] This value was calculated according to the  $1.176(10) \times 10^{-12}$  standard modern  $^{14}\text{C}$  abundance [I. Karlén, U. Olsson, P. Källberg, and S. Kiliççi, *Ark. Geofys.* **6**, 465 (1966)] corrected by a factor of 1.05(1) (see Ref. [18]) to take into account  $^{14}\text{C}^{16}\text{O}_2$  alterations due to two counteracting effects: atmospheric nuclear bomb tests and an atmospheric inlet of  $^{14}\text{C}$ -free  $\text{CO}_2$  coming from the combustion of fossil fuels in the 1950–2010 period.  
 [25] AMS uses  $\text{CO}_2$  gas as an intermediate product to obtain the graphite target tablets from the combustion of the biological sample to be dated.  
 [26] J. Ye, L.-S. Ma, and J. L. Hall, *J. Opt. Soc. Am. B* **15**, 6 (1998).  
 [27] J. B. McManus, M. S. Zahniser, and D. D. Nelson, *Appl. Opt.* **50**, A74 (2011).  
 [28] J. B. McManus, J. H. Shorter, D. D. Nelson, M. S. Zahniser, D. E. Glenn, and R. M. McGovern, *Appl. Phys. B* **92**, 387 (2008).  
 [29] M. Sowa, M. Mürtz, and P. Hering, *J. Breath Res.* **4**, 047101 (2010).  
 [30] G. Maisons, P. Gorrotxategi Carbajo, M. Carras, and D. Romanini, *Opt. Lett.* **35**, 3607 (2010).  
 [31] D. D. Arslanov, S. M. Cristescu, and F. J. M. Harren, *Opt. Lett.* **35**, 3300 (2010).